HHS Public Access

Author manuscript

Oncogene. Author manuscript; available in PMC 2022 May 17.

Published in final edited form as:

Oncogene. 2021 April ; 40(17): 3047–3059. doi:10.1038/s41388-021-01752-2.

A molecular subtype of colorectal cancers initiates independently of epidermal growth factor receptor and has an accelerated growth rate mediated by IL10-dependent anergy

Carolina Mantilla-Rojas[1,2], **Ming Yu**[3,4], **Erica S. Rinella**[3,5], **Rachel M. Lynch**[2,3], **Amie Perry**[2,6], **Jorge Jaimes-Alvarado**[2], **Kathryn R. Anderson**[2], **Estefania Barba**[2], **Evann J. Bourgeois**[2], **Kranti Konganti**[7], **David W. Threadgill**[1,2,7,8,*]

[1]Interdisciplinary Program in Genetics, Texas A&M University; College Station, Texas, 77843, USA

[2]Department of Molecular and Cellular Medicine, Texas A&M University, College Station, TX 77843, USA

[3]Department of Genetics, University of North Carolina, Chapel Hill, NC 27599, USA

[4]Clinical Research Division, Fred Hutchinson Cancer Research Center, Seattle, WA 98109, USA

[5]GeneDx, Gaithersburg, MD 20877, USA

[6]Thompson Bishop Sparks State Diagnostic Laboratory, Auburn AL 36832, USA

[7]Texas A&M Institute for Genome Sciences and Society, Texas A&M University; College Station, TX 77843, USA

[8]Department of Biochemistry & Biophysics and Department of Nutrition, Texas A&M University; College Station, TX 77843, USA

Abstract

Although epidermal growth factor receptor (EGFR)-targeted therapies are approved for colorectal cancer (CRC) treatment, only 15% of CRC patients respond to EGFR inhibition. Here, we show that colorectal cancers (CRC) can initiate and grow faster through an EGFR-independent mechanism, irrespective of the presence of EGFR, in two different mouse models using tissue-specific ablation of *Egfr*. The growth benefit in the absence of EGFR is also independent of *Kras* status. An EGFR-independent gene expression signature, also observed in human CRCs,

*Correspondence: dwt@tamu.edu (D.W.T.).

Author contributions

Conceptualization: CMR, MY, ESR, and DWT
Methodology: CMR, MY, ESR, RML, JJ-A, KRA, EJB, EB, and DWT
Pathology: AP
Data Analysis: CMR, ESR, KK, and DWT
Writing-Original Draft: CMR and DWT
Writing-Reviewing and Editing: MY, ESR, JJ-A., KRA, EJB, EB, and RML
Funding Acquisition: DWT, ESR, and RML.

Supplementary information

Supplementary information accompanies this paper.

Disclosures of Potential Conflicts of Interest

The authors have no competing interests to declare.

revealed that anergy-inducing genes are overexpressed in EGFR-independent polyps, suggesting increased infiltration of anergic lymphocytes promotes an accelerated growth rate that is partially caused by escape from cell-mediated immune responses. Many genes in the EGFR-independent gene expression signature are downstream targets of interleukin 10 receptor alpha (IL10RA). We further show that IL10 is detectable in serum from mice with EGFR-independent colon polyps. Using organoids *in vitro* and *Src* ablation *in vivo*, we show that IL10 contributes to growth of EGFR-independent CRCs, potentially mediated by the well-documented role of SRC in IL10 signaling. Based on these data, we show that the combination of an EGFR inhibitor with an anti-IL10 neutralizing antibody results in decreased cell proliferation in organoids and in decreased polyp size in pre-clinical models harboring EGFR-independent CRCs, providing a new therapeutic intervention for CRCs resistant to EGFR inhibitor therapies.

Keywords

Colorectal cancer; epidermal growth factor receptor; IL10; SRC; anergy

Introduction

The epidermal growth factor receptor (EGFR) was one of the first targets for molecular-targeted therapies [1], and became a popular target for therapeutic strategies designed to treat metastatic colorectal cancer (CRC) [2]. However, over the last two decades, numerous clinical trials showed large differences among CRC patients with only 15% of patients showing a response to EGFR inhibitor therapies [3]. Retrospective subgroup analyses showed that benefits of anti-EGFR therapies are limited to sub-populations of patients. Genetic or epigenetic alterations in proteins involved in regulation of EGFR and downstream pathways, such as KRAS, BRAF, PI3K, and PTEN, partially explain some non-responding cases [4]. Currently, the subgroup of patients whose CRCs are wildtype for *KRAS*, *BRAF*, *PIK3CA*, and expressing normal levels of PTEN have the best response to anti-EGFR therapies [5–7]. Nevertheless, many CRCs remain resistant to anti-EGFR therapies irrespective of mutational status, suggesting the existence of unknown mechanisms capable of influencing treatment effectiveness.

Although numerous factors likely contribute to high levels of resistance to EGFR inhibitors, a lack of constitutional dependency on the EGFR signaling pathway by CRCs has remained unexplored and could explain the lack of clinical response observed for the majority of CRCs. Previous studies using the $Apc^{Min/+}$ mouse model of CRC and either the hypomorphic $Egfr^{wa2}$ allele or pharmaceutical inhibition of EGFR showed that polyp development is greatly reduced with decreased EGFR activity [8, 9]. Nonetheless, a subset of intestinal polyps still arose in these studies, and were larger in the absence of normal EGFR activity. Although these results suggested that a subset of CRCs may arise independently of EGFR activity, these results were also inconclusive since the studies used a hypomorphic *Egfr* allele or pharmacological inhibition, both of which retain measurable EGFR activity and thus are not able to distinguish EGFR independence from variable residual EGFR activity. In this study, we used a conditional knockout allele of *Egfr*

(Egfr^{tm1dwt} also called *Egfr*^{f}) to conclusively demonstrate that colorectal polyps can initiate through an EGFR-independent mechanism in two different mouse models of CRC.

The *Apc*$^{Min/+}$ mouse model has been used for 30 years as a model to study the progression of CRC [10]. This model has phenotypic and genetic similarities to familial adenomatous polyposis (FAP) patients, making it an ideal model to investigate intestinal neoplasia. However, FAP patients account for less than 1% of CRC cases, and the *Apc*$^{Min/+}$ mouse model develops a small number of colon polyps that are generally benign and do not progress to invasive colon cancer [11]. Considering the limitations of the *Apc*$^{Min/+}$ mouse model, in this study we also used a previously described mouse model of sporadic CRC [18]. This model uses conditional inactivation of *Apc* (*Apc*^{tm2Rak} or *Apc*$^{f/f}$) in combination with a conditionally activatable allele of oncogenic *Kras* (*Kras*^{tm4Tyj} or *Kras*$^{LSL/+}$).

Accumulating evidence also suggests that the formation of a tumor microenvironment (TME) enriched in cancer-associated fibroblasts, macrophages, and regulatory T (Treg) cells is a key step in tumor development mediated by chemokines and cytokines [12]. Several studies utilizing mouse models support the requirement of epithelium-derived cytokines, like interleukin 11 (IL11), for the development of CRC [13]. In addition to definitively proving the existence of an EGFR-independent pathway for CRC development, we show that the mechanism for EGFR independence is through IL11 and interleukin 10 (IL10), a TH2 cytokine secreted by almost all leukocytes and intestinal epithelium cells [14–16]. We show that IL10, specifically expressed in EGFR-independent polyps, alters proliferation of organoids derived from EGFR-independent polyps *in vitro* and regulates immune activity by inducing an anergenic state through T-cell infiltration of EGFR-independent polyps *in vivo*. Consistent with known IL10 activities [17, 18], we show that the immune response is modulated by favoring differentiation of monocytes toward M2-like macrophages, which accumulate in the TME. As a proof-of-concept therapy for EGFR-independent CRC, we show that IL10 neutralizing antibodies in combination with small molecule EGFR inhibition blocks growth of EGFR-independent CRCs *in vitro* and *in vivo*.

Results

Intestinal and colonic polyps are fewer in number but larger in size in the absence of EGFR

We and others previously observed that a subset of intestinal polyps in the *Apc*$^{Min/+}$ mouse model still arise, and are larger, in the context of a hypomorphic *Egfr* allele (*Egfr*^{wa2}) or pharmacological EGFR inhibition [8, 9], suggesting the existence of an EGFR-independent mechanism by which polyps can arise. To directly test whether polyps can arise independently of EGFR, we used a conditional knockout allele of *Egfr* (*Egfr*^{tm1Dwt} also called *Egfr*^{f}) [19] in combination with Cre recombinase driven by the villin promoter that is expressed throughout the intestinal epithelia (*Tg(Vil1-Cre)*). At 100 days of age, mice with tissue-specific deletion of *Egfr* (*Apc*$^{Min/+}$, *Egfr*$^{f/f}$, *Tg(Vil1-Cre)*) displayed an 80% reduction in total polyp number compared to littermates with normal levels of EGFR (*Apc*$^{Min/+}$, *Egfr*$^{f/f}$; $p < 0.0001$) (Fig. 1a), similar to what was originally observed with genetic or pharmacologic reduction of EGFR activity [8]. No significant difference in the number of colon polyps was observed in the absence of *Egfr* (Supplementary Fig. 1), although few colonic polyps arose in the *Apc*$^{Min/+}$ model. Also, similar to the original study with reduced

EGFR activity [8], the polyps that developed in the absence of EGFR were significantly larger ($p < 0.05$) than those developing under normal levels of EGFR (Fig. 1b).

Considering the limitations of the $Apc^{Min/+}$ mouse model to recapitulate human colon tumors, we also used a mouse model of inducible CRC to test whether colon polyps can also arise independently of EGFR. Colon polyps developing under normal levels of EGFR ($Egfr^{+/+}$, $Apc^{f/f}$, $Kras^{LSL/+}$) were considered EGFR-dependent, while polyps arising in the absence of EGFR were considered EGFR-independent ($Egfr^{f/f}$, $Apc^{f/f}$, $Kras^{LSL/+}$). We also analyzed mice with a wildtype *Kras* allele carrying $Apc^{f/f}$ ($Egfr^{+/+}$, $Apc^{f/f}$, $Kras^{+/+}$) compared to animals with a combination of $Apc^{f/f}$ and $Egfr^{f/f}$ ($Egfr^{f/f}$, $Apc^{f/f}$, $Kras^{+/+}$). Following focal delivery of a CRE recombinase-expressing adenovirus (AdCre) to the distal colon, colonic polyps arose in the absence of EGFR irrespective of the presence or absence of oncogenic KRAS (Fig. 1c). No polyps developed by inactivating *Apc* alone in the presence of EGFR. Interestingly, mice lacking *Egfr* showed increased polyp penetrance compared to those with *Egfr*, irrespective of *Kras* status. Additionally, despite the focal induction of polyps with AdCre, polyp multiplicity was higher for EGFR-independent polyps than EGFR-dependent polyps ($p < 0.001$) (Fig. 1d).

We assessed the rate of polyp growth by serial colonoscopy every two weeks by comparing the ratio of the polyp and lumen cross-sectional areas (Fig. 1e). The EGFR-independent group showed a significantly higher luminal occlusion until week 15 ($p < 0.05$) (Fig. 1f), reaching occlusion much faster than the EGFR-dependent group. Taken together, these results definitely establish the existence of a subset of colon polyps that arise independent of EGFR and that in the absence of EGFR, polyps are more likely to arise and have an accelerated growth rate irrespective of *Kras* status.

EGFR-independent polyps have a unique gene expression signature

To determine how EGFR-independent polyps can arise in the presence of EGFR, we analyzed RNA from intestinal polyps from $Apc^{Min/+}$, $Egfr^{f/f}$ and $Apc^{Min/+}$, $Egfr^{f/f}$, *Tg(Vil1-Cre)* mice. Hierarchical clustering (Supplementary Fig. 2a) and PCA analysis (Supplementary Fig. 2b) from the transcriptome data demonstrated a clear distinction between $Apc^{Min/+}$, $Egfr^{f/f}$ and $Apc^{Min/+}$, $Egfr^{f/f}$, *Tg(Vil1-Cre)* intestinal polyps. A subset of intestinal polyps from $Apc^{Min/+}$, $Egfr^{f/f}$ mice, with normal levels of EGFR, clustered with $Apc^{Min/+}$, $Egfr^{f/f}$, *Tg(Vil1-Cre)* polyps. The presence of $Apc^{Min/+}$, $Egfr^{f/f}$ that clustered with $Apc^{Min/+}$, $Egfr^{f/f}$, *Tg(Vil1-Cre)* polyps confirmed the existence of an EGFR-independent mechanism of CRC progression even in mice with normal EGFR present. Together, these results suggest that the EGFR-independent pathway is not dependent upon loss of EGFR, but occurs in a subset of polyps upon initiation.

To evaluate whether this unique type of CRC is potentially relevant in humans, we tested human genes orthologous to those in the 1,290 gene mouse EGFR-independent molecular signature using data in the Cancer Genome Atlas (TCGA) database. We found that human CRCs partition into three classes, two of which correspond to EGFR-dependent and independent polyps based on directionality of the gene expression levels (Supplementary Fig. 3a). Similar to the accelerated growth of EGFR-independent polyps in the $Apc^{Min/+}$ model, the majority of human are CRCs predicted to be EGFR-independent based on lower

survival rates (Supplemental Fig. 3b), consistent with the observation that over 80% of human 3D CRC organoids do not respond to EGFR inhibition [20].

Comparative transcriptomics also revealed differential gene expression related to *Egfr* and *Kras* status in the inducible model of CRC (Supplementary Fig. 4a). When compared to their respective adjacent normal tissue, transcriptomic analysis revealed a group of genes that characterize the three polyps types (Supplementary Fig. 4b). Forty-four genes were found to be differentially expressed between EGFR-dependent ($Egfr^{+/+}$, $Apc^{f/f}$, $Kras^{LSL/+}$) and EGFR-independent ($Egfr^{f/f}$, $Apc^{f/f}$, $Kras^{LSL/+}$) colonic polyps (Supplementary Table 1). Up-regulated genes included *Aadac, Sult1a1, Itpka Sult1c2, Bmp3 and Aldh1a*, while downregulated genes included *Ngf, Rnaset2b, Col5a3, and Erdr1*. Ingenuity pathway analyis (IPA) suggested that there are several upstream regulators that determine the EGFR dependency of colon polyps (Supplementary Tables 2–5). Differentially expressed genes are enriched in canonical pathways involving melatonin degradation, serotonin degradation, and dopamine degradation (Supplementary Fig. 5a). The most significant potential upstream molecules associated with the differentially expressed genes were IL10RA (z-score = 3.148, $p = 1.10\times10^{-10}$), HNF1A (z-score = 2.392, $p = 1.09\times10^{-5}$), glucocorticoid (z-score = 1.982, $p = 1.19\times10^{-3}$), and beta-estradiol (z-score = 1.367, $p = 1.69\times10^{-2}$) (Supplementary Table 6). IPA analysis also suggested that the top three enriched signaling networks were dermatological diseases and conditions, organ morphology, small molecule biochemistry (Network 1), lipid metabolism, small molecule biochemistry, vitamin and mineral metabolism (Network 2), and cell to cell signaling interaction, drug metabolism, post-translational modification (Network 3) (Supplementary Fig. 5b). The core nodes in the signaling Network 1 include ERK1/2, MAPK and PI3K complex. For Network 2 and Network 3, the core nodes include IL1B and beta-estradiol, respectively. Analysis of the transcriptome data from $Apc^{Min/+}$, $Egfr^{f/f}$, *Tg(Vil1-Cre)* and $Apc^{Min/+}$, $Egfr^{f/f}$ intestinal polyps, in the absence of *Kras* mutations, also indicated that IL10RA is a common upstream regulator of the differentially expressed genes (Supplementary Table 1).

We validated by quantitative-PCR (qPCR) five common genes (*Aadac*, *Sult1a1, Aldh1a1, Maob, and Sult1c2*) between the top five enriched canonical pathways and the upstream regulator IL10RA (Supplementary Fig. 6). We showed that the transcript levels of *Aadac*, *Sult1a1*, *Aldh1a1* are up-regulated in polyps lacking EGFR, independent of *Kras* status. *Maob* and *Sult1c2* are up-regulated only in polyps lacking EGFR with mutant *Kras*.

EGFR-independent colon polyps escape immune response through IL10-induced anergy

Based on the transcriptomic analysis showing that IL10RA is a common upstream regulator of EGFR-independent polyps, we examined the role of IL10 signaling in EGFR-independent polyp growth by initially measuring *Il10ra* and *Il10* transcriptomic levels in $Egfr^{+/+}$, $Apc^{f/f}$, $Kras^{LSL/+}$ and $Egfr^{f/f}$, $Apc^{f/f}$, $Kras^{LSL/+}$ colon polyps. We did not observe any statistically significant differences in transcript levels of *Il10ra* (Fig. 2a), however we did see an increase in the transcript levels of *Il10* (Fig. 2b) and a well-known downstream target of IL10RA, *Socs3* (Fig. 2c) suggesting that IL10RA is activated in EGFR-independent polyps. Consistent with elevated *Il10* expression in $Egfr^{f/f}$, $Apc^{f/f}$, $Kras^{LSL/+}$ polyps, we also observed a substantial increase in IL10 levels in serum from animals with $Egfr^{f/f}$, $Apc^{f/f}$,

Kras$^{LSL/+}$ colon polyps compared with serum from mice with *Egfr*$^{+/+}$, *Apc*$^{f/f}$, *Kras*$^{LSL/+}$ polyps (Fig. 2d). Increased levels of IL10 in serum have been associated with poor prognosis and lower survival in CRC patients [21, 22].

Because IL10 is known to regulate the differentiation of M2 macrophages [23], we evaluated whether accumulation of tumor infiltrating lymphocytes (TILs) is increased in EGFR-independent polyps. Immunohistochemical evaluation showed that *Egfr*$^{f/f}$, *Apc*$^{f/f}$, *Kras*$^{LSL/+}$ colon polyps exhibited abundant clusters of CD45-positive leukocytes (Supplementary Fig. 7) and total macrophages positive for F4/80 (Fig. 2e–f). When the type of macrophages present in EGFR-independent polyps was analyzed, they were found to be CD163-positive M2 macrophages (Fig. 2g) with lower presence of iNOS-positive M1 macrophages (Fig. 2h). An accumulation of CD3-positive T-cells was observed in both *Egfr*$^{+/+}$, *Apc*$^{f/f}$, *Kras*$^{LSL/+}$ and *Egfr*$^{f/f}$, *Apc*$^{f/f}$, *Kras*$^{LSL/+}$ colon polyps (Supplementary Fig. 6). Based on these results, the combination of EGFR-independence and mutant *Kras* appears to be more important in the formation of the TME than EGFR dependency or *Kras* status alone.

The immunosuppressive cytokine IL10 has been associated with poor prognosis in colon cancer [21, 22, 24]. Although macrophages are involved in anti-tumor defenses, production of IL10 by tumor cells may allow malignant cells to escape cell-mediated immune defenses. In order to determine if IL10 induces an anergic state in T-cell infiltrating EGFR-independent colon polyps, we examined the expression of several anergy-associated genes in EGFR-independent colon polyps compared to adjacent control normal colon tissue and EGFR-dependent polyps (Supplementary Fig. 8). Anergy-inducing genes were activated in T-cell infiltrating EGFR-independent colon polyps, suggesting that in the absence of EGFR, polyps escape the immune system through anergy by increasing IL10 levels.

Consistent with the activation of IL10 signaling in EGFR-independent colon polyps, we showed that the inhibition of Rous sarcoma oncogene (*Src*), a downstream regulator of IL10 signaling, also reduced colon tumorigenesis *in vivo* (Supplementary Fig. 9). We used mice carrying the *Src*^{tm1Sor} targeted mutation to reduce SRC activity in *Apc*$^{Min/+}$ mice. At five-months of age, small intestinal polyp number in *Apc*$^{Min/+}$, *Src*$^{tm1Sor/+}$ mice was reduced 35% compared to *Apc*$^{Min/+}$, *Src*$^{+/+}$ littermates ($p = 0.0167$). In addition, small intestinal polyps were approximately 20% smaller in *Apc*$^{Min/+}$, *Src*$^{tm1Sor/+}$ mice compared to polyps in their *Apc*$^{Min/+}$, *Src*$^{+/+}$ littermates ($p = 0.0133$). To evaluate potential efficacy of EGFR and SRC inhibitor combinatorial therapy, *Apc*$^{Min/+}$, *Src*$^{+/+}$ and *Apc*$^{Min/+}$, *Src*$^{tm1Sor/+}$ mice were treated with the small molecule EGFR inhibitor, AG1478. AG1478 reduced colonic polyp number in *Apc*$^{Min/+}$, *Src*$^{tm1Sor/+}$ mice by 70%, with a cooperative effect when comparing *Apc*$^{Min/+}$, *Src*$^{+/+}$ with *Apc*$^{Min/+}$, *Src*$^{tm1Sor/+}$ mice on AG1478 ($p = 0.0444$). Together these data suggest that IL10 signaling, potentially through SRC activation, promotes an increase in cell proliferation in EGFR-independent colon polyps

IL10 signaling in epithelial cells is required for increased growth rate of EGFR-independent colon polyps

We showed that *Il10* transcripts in colon polyps and IL10 levels in serum are increased in mice with *Egfr*$^{f/f}$, *Apc*$^{f/f}$, *Kras*$^{LSL/+}$ colon polyps. EGFR-independent colon polyps also showed an increase in cell proliferation (Ki67+ cells) when compared with *Egfr*$^{+/+}$, *Apc*$^{f/f}$,

Kras$^{LSL/+}$ polyps (Supplementary Fig. 7). To evaluate the role of IL10 in promoting polyp growth, we performed *in vitro* experiments using colon polyp organoids. Polyp organoids were treated with IL10 or an IL10 neutralizing antibody to evaluate the effect of IL10 signaling on colon polyp growth.

Similar to *in vivo* results, we observed that single-cell suspensions from established *Egfr*$^{f/f}$, *Apc*$^{f/f}$, *Kras*$^{LSL/+}$ organoids grew faster and showed higher cell proliferation than *Egfr*$^{+/+}$, *Apc*$^{f/f}$, *Kras*$^{LSL/+}$ organoids at 24 hours after seeding (Fig. 3a). We also found increased levels of IL10 in the conditioned media of *Egfr*$^{f/f}$, *Apc*$^{f/f}$, *Kras*$^{LSL/+}$ organoids (Fig. 3a), suggesting that epithelial cells were the source of elevated serum IL10 *in vivo*. To test the effect of IL10 on cell proliferation, cells were seeded and after serum starvation for 12 hours, organoids were treated with mouse recombinant IL10 protein, which significantly increased cell proliferation of *Egfr*$^{+/+}$, *Apc*$^{f/f}$, *Kras*$^{LSL/+}$ organoids in a dose-dependent manner (Fig. 3b). This effect was not observed in EGFR-independent *Egfr*$^{f/f}$, *Apc*$^{f/f}$, *Kras*$^{LSL/+}$ organoids that presumably are already producing sufficient levels of IL10 for maximal growth. Conversely, proliferation was attenuated in *Egfr*$^{f/f}$, *Apc*$^{f/f}$, *Kras*$^{LSL/+}$ organoids treated with an IL10 neutralizing antibody (Fig. 3c), while EGFR-dependent *Egfr*$^{+/+}$, *Apc*$^{f/f}$, *Kras*$^{LSL/+}$ organoids showed increased growth and IL10 levels (Supplementary Fig. 10) in the media after treatment with EGFR inhibitor AG1478 (Fig. 3d). Furthermore, a cooperative effect of EGFR inhibitor and IL10 neutralizing antibody on organoid size was observed irrespective of EGFR status (Fig. 3e), suggesting that targeting both pathways could overcome the activation of compensatory pathways and be therapeutically beneficial in both EGFR-dependent and independent CRC. Together, these data confirm that IL10 is required for EGFR-independent cell proliferation and its presence can increase growth of EGFR-dependent polyps.

To evaluate the potential therapeutic utility of anti-IL10 neutralizing antibody treatment on CRC *in vivo*, mice with *Egfr*$^{+/+}$, *Apc*$^{f/f}$, *Kras*$^{LSL/+}$ and *Egfr*$^{f/f}$, *Apc*$^{f/f}$, *Kras*$^{LSL/+}$ colon polyps were administrated either anti-IL10 neutralizing antibody or vehicle (PBS). Confirming the *in vitro* results, anti-IL10 antibody administration significantly reduced *Egfr*$^{f/f}$, *Apc*$^{f/f}$, *Kras*$^{LSL/+}$ colon polyp size, with one polyp disappearing completely upon anti-IL10 treatment, compared to control mice (Fig. 4). There was no effect of anti-IL10 treatment on polyps from *Egfr*$^{+/+}$, *Apc*$^{f/f}$, *Kras*$^{LSL/+}$ mice, indicating a potential therapeutic avenue for EGFR-independent polyps.

Discussion

In this study, we definitively established the existence of a subtype of colon polyps that arise independently of EGFR and demonstrated its correlation with a more aggressive growth phenotype using two independent mouse models. We also showed that increased IL10 contributes to elevated growth of EGFR-independent polyps by direct action on transformed epithelial cells and via anergic T-cells in the TME. These data led to a model whereby IL10 upregulation, possibly via SRC, promotes CRC development in the absence of EGFR (Fig. 5).

The observation that a majority of CRC patients do not respond to anti-EGFR therapeutics, despite promising pre-clinical data, is a major hindrance to the success of these agents. Previous reports using genetic and pharmacological inhibition to reduce [8], but not eliminate EGFR activity, were inconclusive as to whether colon polyps can arise and grow independently of EGFR activity. The previous study could not distinguish EGFR independence from variable residual EGFR activity. In the current study, we took advantage of a conditional knockout allele of *Egfr* to definitely prove that a subset of intestinal and colon polyps arise independently of EGFR signaling. Our genetic approach demonstrates that despite having greatly reduced polyp numbers, $Apc^{Min/+}$, $Egfr^{f/f}$, *Tg(Vil1-Cre)* mice with intestinal-epithelia specific *Egfr* deletion still develop polyps showing that these polyps grow in an EGFR-independent manner. We also show that under normal levels of EGFR, a subset of intestinal polyps arise with a similar gene expression profile to those without EGFR, suggesting that these polyps might have a constitutive mechanism to develop independent of EGFR activity. Unexpectedly, the absence of EGFR in these polyps enhances their growth. Therefore, some CRCs are likely to not respond to EGFR inhibitor therapies since they do not rely on EGFR for survival or proliferation. In contrast, targeting EGFR would be most effective for those cancers that are dependent upon EGFR signaling. Based on expression of genes orthologous to those in the mouse EGFR-independent signature, a subset of human CRCs appears to be EGFR-independent and patients with these CRCs have a lower survival rate.

Although mechanistically different, differential response to EGFR inhibition is well documented in non-small-cell lung carcinoma (NSCLC), where patients harboring EGFR activating mutations exhibit dramatic clinical responses to gefitinib [25–27]. Additionally, a preclinical model of CRC in mice showed that even in the absence of *Kras* mutation, EGFR status influences the development of colon polyps by activating compensatory pathways like EGFR-MET interaction after treatment with cetuximab [28]. In addition, it has been shown that IL10 activates the MET/STAT3 signaling pathway regulating proliferation and invasion in gastric cancer cells [29]. This data provides evidence of the possible role of IL10 signaling in the resistance to current anti-EGFR treatment.

Transcriptomic analysis predicted that IL10RA signaling was upregulated in EGFR-independent intestinal and colon polyps, and increased transcript levels of *Il10* and *Socs3* confirmed that IL10RA signaling was activated in EGFR-independent colon polyps. Previous studies in lung cancer reported that IL10 increased the levels of phospho-SRC in a dose dependent manner, promoting increase in tumor cell proliferation [24, 30]. Accumulating evidence suggests that SRC also contributes to cancer development and may be a target in the treatment of CRC [31]. SRC is a non-receptor tyrosine kinase that is activated in human colon, breast, liver, lung, and pancreatic cancers, and is increased in polyps arising in $Apc^{Min/+}$ mice [32]. Supporting an important role for SRC, inhibition of SRC activity reduces growth of human CRC cells as well as tumor growth in xenograft models [33]. In the current study, we demonstrated that the inhibition of SRC activity reduces tumorigenesis *in vivo*, and that combining SRC and EGFR inhibition is more efficacious than inhibiting either kinase alone. These data support the previous results that an EGFR-independent mechanism could use IL10 and its SRC signaling to promote a more aggressive development of colon tumor.

The activation of IL10 signaling correlates with previous studies suggesting that IL10 promotes cancer development by inhibiting anti-tumor immune responses. Specifically, IL10 can impair the activation of cytotoxic T lymphocytes (CTLs) and Th1 CD4+ cells [34], and can inhibit the cytolytic activity of natural killer cells and CTLs [35], which are responsible for the immune surveillance of cancer. We found that IL10 was increased in two different mouse models of CRC lacking *Egfr* (*Apc*$^{Min/+}$*, Egfr*$^{f/f}$*, Tg(Vil1-Cre)*; *Egfr*$^{f/f}$, *Apc*$^{f/f}$*, Kras*$^{LSL/+}$; and *Egfr*$^{f/f}$, *Apc*$^{f/f}$*, Kras*$^{+/+}$). In addition, activation of anergy-associated genes in EGFR-independent colon polyps confirmed that IL10 may act as a suppressor of the immune system. We also confirmed that *Egfr*$^{f/f}$, *Apc*$^{f/f}$*, Kras*$^{LSL/+}$ polyps showed an increased infiltration of M2-type macrophages acting in favor of polyp progression and stimulating tumor growth [36]. Treatment with an IL10 neutralizing antibody reduced cell proliferation and size of EGFR-independent polyps *in vitro* and *in vivo*. Furthermore, several studies have shown that late-stage CRC patients had higher IL10 expression, and patients with higher IL10 levels had lower survival rates [21, 22]. Although the *in vivo* role of IL10 in colon cancer has not been previously elucidated, IL10 expression by tumor-associated macrophages has been correlated with a poor prognosis [24]. In this study we showed that IL10 serum levels were highly increased in mice with EGFR-independent colon polyps. However, the influence of IL10 on tumor development is still controversial because communication between the tumor microenvironment and tumor cells is critical for cancer development. An experimental model capable of mimicking the tumor environment is needed to elucidate the role that IL10 has on cancer progression. Although it remains unclear whether cancer cells secrete IL10 and whether IL10 plays a role in the aggressiveness and malignancy of cancer cells, our organoid study showed that epithelial cells do secrete measurable levels of IL10.

Based on our data, we suggest that EGFR-independent colonic polyps show increase levels of IL10 that activates IL10RA signaling (Fig. 5). The activation of IL10RA might increase unrecognized compensatory signaling pathways in the absence of EGFR. The combinatorial effect of EGFR and IL10 inhibition indicates that the compensatory pathways is inhibited by these two treatments. Finally, because IL10 inhibition decreases cell proliferation and polyp size *in vivo*, the future development of anti-IL10 treatment in combination with anti-EGFR will be of benefit to improving CRC therapies.

Materials and methods

Animal experiments

All animal studies were conducted under protocols approved by the Texas A&M University Institution Animal Care and Use Committee guidelines. C57BL/6J (B6)-*Apc*$^{Min/+}$ [37] and B6.129S7- *Src*^{tm1Sor} [38] were obtained from The Jackson Laboratory (Bar Harbor, ME). B6;D2-*Tg(Vil-cre)20Syr* [39] and B6.129-*Kras*^{tm4Tyj} [40] were obtained from NCI-Frederick. *Apc*^{tm2Rak} [41] mice were obtained from the International Mouse Strain Resources. We previously generated B6.129- *Egfr*^{tm1dwt} [19]. All strains were crossed for at least 10 generations to the B6 background. Mice were housed five per cage, fed Purina Mills Lab Diet 2919 and maintained at 22° under a 12-hr light cycle. Mice were euthanized by CO_2 asphyxiation for tissue collection.

Crosses were set up in four cages using trios of two females *Egfr*$^{f/+}$, *Apc*$^{Min/+}$ and one male *Egfr*$^{f/+}$, *Apc*$^{Min/+}$. Over six months, littermates were genotyped and, 37 male and 38 female *Egfr*$^{f/f}$, *Apc*$^{Min/+}$ mice and 50 male and 50 female *Egfr*$^{+/+}$, *Apc*$^{Min/+}$ mice were euthanized at 100 days of age to evaluate the effect of EGFR in intestinal tumorigenesis. The number of animals was based on the prediction that 10–20% of polyps in animals with normal levels of *Egfr* would be transcriptionally similar to *Egfr* deficient polyps.

Crosses were set up in four cages using trios of two females *Egfr*$^{f/+}$, *Apc*$^{f/f}$, *Kras*$^{LSL/+}$ *and* one male *Egfr*$^{f/+}$, *Apc*$^{f/f}$, *Kras*$^{+/+}$, littermates were genotyped and 90 mice allocated to the following groups. The number of animals per group was estimated using JMP based on α-value of 0.05 and a desired power of 0.8: 5 females and 5 males *Egfr*$^{+/+}$, *Apc*$^{f/f}$, *Kras*$^{+/+}$; 15 females and 15 males *Egfr*$^{f/f}$, *Apc*$^{f/f}$, *Kras*$^{+/+}$; 10 females and 10 males *Egfr*$^{+/+}$, *Apc*$^{f/f}$, *Kras*$^{LSL/+}$; and 15 females and 15 males *Egfr*$^{f/f}$, *Apc*$^{f/f}$, *Kras*$^{LSL/+}$. Eight cohorts of 12 (3-month-old) mice were randomized in each cohort, with equal representation of each genotype used to locally induce colon polyps using the non-surgical exposure of AdCre described below. Animals that developed anal prolapse and met euthanasia criteria were excluded from transcriptomic analysis.

Src$^{tm1Sor/+}$ females were crossed with *Apc*$^{Min/+}$ males to generate *Apc*$^{Min/+}$ *Src*$^{+/+}$ and *Apc*$^{Min/+}$ *Src*$^{tm1Sor/+}$. Mice were randomly assigned to controls or the AG1478 EGFR inhibitor (LC Labs) treatment group. The number of mice were equally split by sex and included: 19 *Apc*$^{Min/+}$ *Src*$^{+/+}$; 24 *Apc*$^{Min/+}$ *Src*$^{tm1Sor/+}$; 19 *Apc*$^{Min/+}$ *Src*$^{+/+}$ treated with 144mg/kg AG1478; and 24 *Apc*$^{Min/+}$ *Src*$^{tm1Sor/+}$ treated with 144mg/kg AG1478.

Genotyping

Mice were genotyped for the *Apc*^{Min} allele as previously described [8]. Mice were genotyped for the *Egfr*^{tm1Dmt} allele as previously described [19]. Mice were genotyped using PCR with the primers described below:

Vil-Cre

Cre-S1, 5’ - GTGATGAGGTTCGCAAGAAC

Cre-AS1, 5’ - AGCATTGCTGTCACTTGGTC

Kras^{tm4Tyj}

K004, 5’ - GTCGACAAGCTCATGCGGGTG

K005, 5’ - AGCTAGCCACCATGGCTTGAGTAAGTCTGCA

K006, 5’ - CCTTTACAAGCGCACGCAGACTGTAGA

Apc^{tm2Rak}

APC-Int12-F2, 5’ - GAGAAACCCTGTCTCGAAAAAA

APC-Int12-R2, 5’ - AGTGCTGTTTCTATGAGTCAAC

Src^{tm1Sor}

0791, 5’ - CGCTTCCTCGTCCTTTACGGTAT

14275, 5’ - TCCTAAGGTGCCAGCAATTC

oIMR3129, 5’ - GAGTTGAAGCCTCCGAAGAG

Non-surgical exposure to AdCre virus

Polyethylene tubing (I.D. 1.4 mm, O.D. 1.90 mm; Becton Dickinson, Sparks, MD) was cut to sizes appropriate for mice (10 cm). A 1 cm window was notched into the tubing and the end of the tubing was closed with edges being rounded to avoid perforation of the bowel. Marks corresponding to 1 cm intervals were made on the tubing. A longitudinal stripe was also applied corresponding to the orientation of the window. Mice were anesthetized using 2% isoflurane. The colon was irrigated with phosphate buffered saline (PBS). A narrow ribbon of GelFoam (Pharmacia and Upjohn, NY, NY) was inserted into the window cut into the polyethylene tube. 200 μL of 0.05% trypsin (Hyclone, Logan, VT) was injected into the tubing and inserted into the mouse colon at the desired depth and radial orientation. After 10 minutes, the slotted tube was removed and a soft flocked brush (Puritan Purflock Ultra Flocked 25–3316-U) was introduced at the same intraluminal location. The brush was then used to abrade the epithelium for up to 3 minutes. After PBS irrigation, a slotted tubing containing GelFoam was then filled with 200μL PBS containing 10^9 PFU of Cre recombinase-expressing adenovirus (AdCre) (Ad5CMVCre and Ad5CMVEmpty, University of Iowa Gene Transfer Vector Core, IA). After 30 minutes of incubation, the tubing was removed. Owing to the anatomical limitations of the mouse, only the most distal half of the colon (~4 cm) could be inoculated in this way. Mice were given Banamine for analgesia and recovered quickly after the procedure. Induction with AdCre was performed in nine different cohorts. Each cohort had a group of mice representing each of the genotypes in the study.

Murine colonoscopy

Mice were anesthetized using 2% isoflurane and the colons were flushed with PBS. The Coloview System was used to monitor polyp formation and growth in the distal half of the colon every two weeks as previously described (Karl Storz, Goleta, CA) [42]. ImageJ analysis was utilized to measure the percent lumen occlusion as previously described [43].

Mouse IL10 neutralizing antibody treatment

For inhibiting IL10 *in vivo*, five mice per genotype (*Egfr*$^{f/f}$, *Apc*$^{f/f}$, *Kras*$^{LSL/+}$, and *Egfr*$^{+/+}$, *Apc*$^{f/f}$, *Kras*$^{LSL/+}$) with established AdCre-induced colonic polyps were monitored for four months. Intraperitoneally (IP) injection with the anti-IL10 was administered (200μg/mouse at the beginning of the treatment; 100μg/mouse and 20μg/mouse injections were IP administrated once/week with two days between injections for four weeks) and PBS as control. After treatment animas were sacrificed, and polyp measurements were taken to quantify treatment effects.

Macroadenoma count

The polyp number and diameter were measured for the entire length of the small intestine and colon using a dissecting microscope and in-scope micrometer at 5x magnification. The smallest polyps that can be counted are approximately 0.3 mm in diameter. Polyp scoring was performed without knowledge of genotype by the investigator. Changes in polyp growth

rate were recorded grossly as polyp size. In addition to polyp size, polyps were carefully scored based on number and location along the gastro-intestinal (GI) tract.

Histology and hematoxylin and eosin (H&E) staining

Intestinal tissues or colon samples were collected and fixed in 10% neutral buffered formalin. The processed tissues were embedded in paraffin and sectioned (7 μm). Every 50 μm, sections were taken and stained with H&E.

Colon polyps were deparaffinized in xylene followed by rehydration in 100%, 90%, and 70% ethanol and distilled water. The slides were then incubated in fresh hematoxylin (Merck, Darmstadt, Germany) for 5 min and washed in distilled water, followed by incubation in acidified eosin solution (Sigma, Deisenhofen, Germany) for 1 min and washing. Finally, the slides were dehydrated in 90% and 100% ethanol, air dried, and mounted. The H&E stained colon sections were assessed by a pathologist (A.P.) for differentiation of polyp tissue from non-polyp tissue. Sections from 5 different animals per genotype were analyzed to generate SEM.

Immunohistochemistry

Immunohistochemical procedures were performed as described [44]. Antigen-retrieval was performed by boiling for 20 min in citrate buffer, pH 6.0. Sections were treated with 0.3% hydrogen peroxide in PBS for 30 min, washed in PBS, blocked in PBS plus 3% specific serum and 0.1% Triton X- 100, and then incubated with primary antibodies and HRP-conjugated specific anti-rabbit secondary antibody (Vector Laboratories, Inc). Antigen-antibody complexes were detected with DAB peroxidase substrate kit (Vector Laboratories, Burlingame, CA) according to the manufacturer's protocol. Suppliers for primary antibodies were Abcam, (CD163-ab182422, iNOS-ab15323, Ki67-ab15580, Tunel Assay Kit-ab206386); Santa Cruz Biotechnology, (CD3-sc-1127); Biolegend, Inc (F4/80-BM8), eBioscience, (CD45-14-0451). The total number of cells and all the positively stained cells in polyp area of the core was counted using Fiji and expressed as a percentage of the total number of cells in the polyp core. Sections from five different animals per genotype were analyzed to generate SEM.

Intestinal organoids

Epithelial-only intestinal minigut cultures from freshly isolated $Egfr^{+/+}$, $Apc^{f/f}$, $Kras^{LSL/+}$ and $Egfr^{f/f}$, $Apc^{f/f}$, $Kras^{LSL/+}$ mouse colonic polyps were established essentially as described previously [45]. Crypts were isolated by calcium chelation and mechanical agitation, then embedded in Matrigel (Corning™ Matrigel™ GFR Membrane Matrix, ThermoFisher CB40230C) droplets with N2 and B27 supplements (ThermoFisher 17502001 and 17504001, respectively). Once established, cultures were broken up by adding 0.25% of trypsin and incubating for 10 minutes. Single cell suspensions of 2000 cells/well were allowed to grow for 24 hours to test differences in cell proliferation. Because $Egfr^{f/f}$, $Apc^{f/f}$, $Kras^{LSL/+}$ organoids grow faster and show higher cell proliferation at 24h after seeding than $Egfr^{+/+}$, $Apc^{f/f}$, $Kras^{LSL/+}$, cells were allowed to grow under serum starvation conditions for 12h to ensure similar number of cells at time of treatment. To evaluate cell proliferation of the organoids, treatment with mouse IL10 recombinant protein,

eBioscience™ (ThermoFisher 14-8101-62), IL10 neutralizing antibody (Clone JES052A5 from R&D MAB417), or EGFR inhibitor AG1478 (LC Labs) was left for an additional 72 hours. A range of four concentrations of each compound was exposed to 3D organoids: mouse recombinant IL10 (5, 10, 20 and 30 ng/ml), IL10 neutralizing antibody (0.5, 1, 2 and 3 ug/ml), EGFR inhibitor AG1478 (0.02, 0.1, 0.5, and 1 mM). On the same plate a medium control and a DMSO control were included. Cell proliferation was measured using CyQUANT™ Cell Proliferation Assay Kit for cells in culture (ThermoFisher C7026). The fluorescent signal was quantified using a microplate reader (Cytation4 BioteK) with excitation at 485 nm and emission detection at 530 nm. Every condition was repeated in three wells per experiment and three times in independent tests. RNA from organoids was isolated using PicoPure™ RNA Isolation Kit (ThermoFisher KIT0214).

Enzyme-linked immunosorbent assay (ELISA)

IL10 concentration in mouse serum was measured using IL10 Mouse Instant ELISA™, (ThermoFisher BMS614INDT). The measurement was performed according to the manufacturer's instructions.

Transcriptomic analysis

A total of three sequencing runs were performed to sequence 56 samples on NextSeq 500 sequencing instrument at Texas A&M Institute for Genome Sciences and Society Molecular Genomics Core using high output kit v2. A total of 1.5 billion 75 bp single-end reads were checked for adapter sequences and low-quality bases using Trimmomatic [46], resulting in approximately 1.4 billion filtered reads (96%). RNA-Seq reads were aligned to mouse assembly mm10 using HISAT2 version 2.0.5 [47] with an overall mapping rate of approximately 97%. Raw gene counts were generated with feature Counts package [48], while discarding ambiguous read mappings. Normalized read counts and gene expression tests were performed using DESeq2 [49] following recommended guidelines by the authors. Ingenuity Pathway Analysis (IPA, Qiagen) was used to analyzed differentially expressed genes between the different groups. RNAseq data was deposited in NIH: BioProject ID PRJNA635118.

Data in the Cancer Genome Atlas (TCGA) database was obtained through proper permissions. RNAseq data from 512 patients designated as TCGA-COAD (Colorectal Adenocarcinoma) was downloaded using the TCGAbiolinks R package [50]. Counts were catalogued at TCGA as generated by the HTSeq package [51]. Filtering was performed to consider patient data where each patient record was designated with "Primary_Tumor" metadata column resulting in a total raw count set for all genes in the orthologous list. The genes were used to perform differential expression analysis using DESeq2 [49].

Quantitative real time PCR

Genes with significant changes in expression between EGFR-dependent and independent polyps, based on ANOVA analysis, were confirmed by qRT-PCR. cDNA was synthesized from total RNA from each polyp using the QuantiTect Reverse Transcription Kit (Qiagen 205314). PCR reactions were set up in 96-well plates, all samples were run in triplicate. Analysis was performed on a LightCycler 96 Thermocycler (Roche) using LightCycler 480

Sybr Green I Master reaction mix. Specific primers were designed to amplify a fragment from the genes (Supplementary Table 7).

Statistics

The nonparametric Mann–Whitney U two-sided test was used to analyze polyp data. To compare the statistical difference between 2 groups, unpaired student's *t* test was used. P-values less than 0.05 was considered as significantly different.

Supplementary Material

Refer to Web version on PubMed Central for supplementary material.

Acknowledgements

This work was supported by fellowships F31 AT002835 (ESR), F32 CA168301 (RML), T32 OD011083 (AP), and by NIH grants R01 CA092479 (DWT), NIEHS P30 ES029067, and the Tom and Jean McMullin Chair of Genetics (DWT). We thank members of the Threadgill lab for constructive criticism on manuscript drafts; Dr. Andrew Hillhouse and the Texas A&M Institute for Genome Sciences and Society's (TIGSS) Molecular Genomics Core for RNAseq data generation; and Kristen Hanneman for mouse husbandry. The results published here are in whole or part based upon data generated by The Cancer Genome Atlas managed by the NCI and NHGRI. Information about TCGA can be found at http://cancergenome.nih.gov.

Availability of data and materials

The datasets supporting the conclusions of this article are available within the article, its supplemental files, and from the corresponding author upon request. The high-throughput sequencing data are deposited in GEO.

References

1. Masui H, Kawamoto T, Sato JD, Wolf B, Sato G, Mendelsohn J. Growth inhibition of human tumor cells in athymic mice by anti-epidermal growth factor receptor monoclonal antibodies. Cancer Res 1984; 44: 1002–1007. [PubMed: 6318979]
2. Martinelli E, De Palma R, Orditura M, De Vita F, Ciardiello F. Anti-epidermal growth factor receptor monoclonal antibodies in cancer therapy. Clin Exp Immunol 2009; 158: 1–9.
3. Yang YH, Lin JK, Chen WS, Lin TC, Yang SH, Jiang JK et al. Comparison of cetuximab to bevacizumab as the first-line bio-chemotherapy for patients with metastatic colorectal cancer: superior progression-free survival is restricted to patients with measurable tumors and objective tumor response--a retrospective study. J Cancer Res Clin Oncol 2014; 140: 1927–1936. [PubMed: 24934725]
4. Martins M, Mansinho A, Cruz-Duarte R, Martins SL, Costa L. Anti-EGFR Therapy to Treat Metastatic Colorectal Cancer: Not for All. Adv Exp Med Biol 2018; 1110: 113–131. [PubMed: 30623369]
5. De Roock W, Claes B, Bernasconi D, De Schutter J, Biesmans B, Fountzilas G et al. Effects of KRAS, BRAF, NRAS, and PIK3CA mutations on the efficacy of cetuximab plus chemotherapy in chemotherapy-refractory metastatic colorectal cancer: a retrospective consortium analysis. Lancet Oncol 2010; 11: 753–762. [PubMed: 20619739]
6. De Roock W, De Vriendt V, Normanno N, Ciardiello F, Tejpar S. KRAS, BRAF, PIK3CA, and PTEN mutations: implications for targeted therapies in metastatic colorectal cancer. Lancet Oncol 2011; 12: 594–603. [PubMed: 21163703]
7. Karapetis CS, Jonker D, Daneshmand M, Hanson JE, O'Callaghan CJ, Marginean C et al. PIK3CA, BRAF, and PTEN status and benefit from cetuximab in the treatment of advanced colorectal

cancer--results from NCIC CTG/AGITG CO.17. Clin Cancer Res 2014; 20: 744–753. [PubMed: 24218517]

8. Roberts RB, Min L, Washington MK, Olsen SJ, Settle SH, Coffey RJ et al. Importance of epidermal growth factor receptor signaling in establishment of adenomas and maintenance of carcinomas during intestinal tumorigenesis. Proc Natl Acad Sci U S A 2002; 99: 1521–1526. [PubMed: 11818567]
9. Torrance CJ, Jackson PE, Montgomery E, Kinzler KW, Vogelstein B, Wissner A et al. Combinatorial chemoprevention of intestinal neoplasia. Nat Med 2000; 6: 1024–1028. [PubMed: 10973323]
10. Ren J, Sui H, Fang F, Li Q, Li B. The application of Apc(Min/+) mouse model in colorectal tumor researches. J Cancer Res Clin Oncol 2019; 145: 1111–1122. [PubMed: 30887153]
11. Jackstadt R, Sansom OJ. Mouse models of intestinal cancer. J Pathol 2016; 238: 141–151. [PubMed: 26414675]
12. Parseghian CM, Napolitano S, Loree JM, Kopetz S. Mechanisms of Innate and Acquired Resistance to Anti-EGFR therapy: A Review of Current Knowledge with a Focus on Rechallenge Therapies. Clin Cancer Res 2019.
13. Putoczki TL, Thiem S, Loving A, Busuttil RA, Wilson NJ, Ziegler PK et al. Interleukin-11 is the dominant IL-6 family cytokine during gastrointestinal tumorigenesis and can be targeted therapeutically. Cancer Cell 2013; 24: 257–271. [PubMed: 23948300]
14. Wolk K, Kunz S, Asadullah K, Sabat R. Cutting edge: immune cells as sources and targets of the IL-10 family members? J Immunol 2002; 168: 5397–5402. [PubMed: 12023331]
15. Fiorentino DF, Bond MW, Mosmann TR. Two types of mouse T helper cell. IV. Th2 clones secrete a factor that inhibits cytokine production by Th1 clones. J Exp Med 1989; 170: 2081–2095. [PubMed: 2531194]
16. Moore KW, de Waal Malefyt R, Coffman RL, O'Garra A. Interleukin-10 and the interleukin-10 receptor. Annu Rev Immunol 2001; 19: 683–765. [PubMed: 11244051]
17. Jackute J, Zemaitis M, Pranys D, Sitkauskiene B, Miliauskas S, Vaitkiene S et al. Distribution of M1 and M2 macrophages in tumor islets and stroma in relation to prognosis of non-small cell lung cancer. BMC Immunol 2018; 19: 3. [PubMed: 29361917]
18. Solinas G, Germano G, Mantovani A, Allavena P. Tumor-associated macrophages (TAM) as major players of the cancer-related inflammation. J Leukoc Biol 2009; 86: 1065–1073. [PubMed: 19741157]
19. Lee TC, Threadgill DW. Generation and validation of mice carrying a conditional allele of the epidermal growth factor receptor. Genesis 2009; 47: 85–92. [PubMed: 19115345]
20. Schumacher D, Andrieux G, Boehnke K, Keil M, Silvestri A, Silvestrov M et al. Heterogeneous pathway activation and drug response modelled in colorectal-tumor-derived 3D cultures. PLoS Genet 2019; 15: e1008076. [PubMed: 30925167]
21. Zhao S, Wu D, Wu P, Wang Z, Huang J. Serum IL-10 Predicts Worse Outcome in Cancer Patients: A Meta-Analysis. PLoS One 2015; 10: e0139598. [PubMed: 26440936]
22. Mager LF, Wasmer MH, Rau TT, Krebs P. Cytokine-Induced Modulation of Colorectal Cancer. Front Oncol 2016; 6: 96. [PubMed: 27148488]
23. Saqib U, Sarkar S, Suk K, Mohammad O, Baig MS, Savai R. Phytochemicals as modulators of M1-M2 macrophages in inflammation. Oncotarget 2018; 9: 17937–17950. [PubMed: 29707159]
24. Herbeuval JP, Lelievre E, Lambert C, Dy M, Genin C. Recruitment of STAT3 for production of IL-10 by colon carcinoma cells induced by macrophage-derived IL-6. J Immunol 2004; 172: 4630–4636. [PubMed: 15034082]
25. Lynch TJ, Bell DW, Sordella R, Gurubhagavatula S, Okimoto RA, Brannigan BW et al. Activating mutations in the epidermal growth factor receptor underlying responsiveness of non-small-cell lung cancer to gefitinib. N Engl J Med 2004; 350: 2129–2139. [PubMed: 15118073]
26. Paez JG, Janne PA, Lee JC, Tracy S, Greulich H, Gabriel S et al. EGFR mutations in lung cancer: correlation with clinical response to gefitinib therapy. Science 2004; 304: 1497–1500. [PubMed: 15118125]

27. Pao W, Miller VA, Venkatraman E, Kris MG. Predicting sensitivity of non-small-cell lung cancer to gefitinib: is there a role for P-Akt? J Natl Cancer Inst 2004; 96: 1117–1119. [PubMed: 15292378]
28. Troiani T, Martinelli E, Napolitano S, Vitagliano D, Ciuffreda LP, Costantino S et al. Increased TGF-alpha as a mechanism of acquired resistance to the anti-EGFR inhibitor cetuximab through EGFR-MET interaction and activation of MET signaling in colon cancer cells. Clin Cancer Res 2013; 19: 6751–6765. [PubMed: 24122793]
29. Chen L, Shi Y, Zhu X, Guo W, Zhang M, Che Y et al. IL10 secreted by cancerassociated macrophages regulates proliferation and invasion in gastric cancer cells via cMet/STAT3 signaling. Oncol Rep 2019; 42: 595–604. [PubMed: 31233202]
30. Hsu TI, Wang YC, Hung CY, Yu CH, Su WC, Chang WC et al. Positive feedback regulation between IL10 and EGFR promotes lung cancer formation. Oncotarget 2016; 7: 20840–20854. [PubMed: 26956044]
31. Warmuth M, Damoiseaux R, Liu Y, Fabbro D, Gray N. SRC family kinases: potential targets for the treatment of human cancer and leukemia. Curr Pharm Des 2003; 9: 2043–2059. [PubMed: 14529415]
32. Moran AE, Hunt DH, Javid SH, Redston M, Carothers AM, Bertagnolli MM. Apc deficiency is associated with increased Egfr activity in the intestinal enterocytes and adenomas of C57BL/6J-Min/+ mice. J Biol Chem 2004; 279: 43261–43272. [PubMed: 15294912]
33. Golas JM, Lucas J, Etienne C, Golas J, Discafani C, Sridharan L et al. SKI-606, a Src/Abl inhibitor with in vivo activity in colon tumor xenograft models. Cancer Res 2005; 65: 5358–5364. [PubMed: 15958584]
34. Pizarro TT, Arseneau KO, Cominelli F. Lessons from genetically engineered animal models XI. Novel mouse models to study pathogenic mechanisms of Crohn's disease. Am J Physiol Gastrointest Liver Physiol 2000; 278: G665–669. [PubMed: 10801257]
35. Kamizato M, Nishida K, Masuda K, Takeo K, Yamamoto Y, Kawai T et al. Interleukin 10 inhibits interferon gamma- and tumor necrosis factor alpha-stimulated activation of NADPH oxidase 1 in human colonic epithelial cells and the mouse colon. J Gastroenterol 2009; 44: 1172–1184. [PubMed: 19714290]
36. Edin S, Wikberg ML, Dahlin AM, Rutegard J, Oberg A, Oldenborg PA et al. The distribution of macrophages with a M1 or M2 phenotype in relation to prognosis and the molecular characteristics of colorectal cancer. PLoS One 2012; 7: e47045. [PubMed: 23077543]
37. Moser AR, Mattes EM, Dove WF, Lindstrom MJ, Haag JD, Gould MN. ApcMin, a mutation in the murine Apc gene, predisposes to mammary carcinomas and focal alveolar hyperplasias. Proc Natl Acad Sci U S A 1993; 90: 8977–8981. [PubMed: 8415640]
38. Soriano P, Montgomery C, Geske R, Bradley A. Targeted disruption of the c-src proto-oncogene leads to osteopetrosis in mice. Cell 1991; 64: 693–702. [PubMed: 1997203]
39. el Marjou F, Janssen KP, Chang BH, Li M, Hindie V, Chan L et al. Tissue-specific and inducible Cre-mediated recombination in the gut epithelium. Genesis 2004; 39: 186–193. [PubMed: 15282745]
40. Jackson EL, Willis N, Mercer K, Bronson RT, Crowley D, Montoya R et al. Analysis of lung tumor initiation and progression using conditional expression of oncogenic K-ras. Genes Dev 2001; 15: 3243–3248. [PubMed: 11751630]
41. Kuraguchi M, Wang XP, Bronson RT, Rothenberg R, Ohene-Baah NY, Lund JJ et al. Adenomatous polyposis coli (APC) is required for normal development of skin and thymus. PLoS Genet 2006; 2: e146. [PubMed: 17002498]
42. Becker C, Fantini MC, Wirtz S, Nikolaev A, Kiesslich R, Lehr HA et al. In vivo imaging of colitis and colon cancer development in mice using high resolution chromoendoscopy. Gut 2005; 54: 950–954. [PubMed: 15951540]
43. Hung KE, Maricevich MA, Richard LG, Chen WY, Richardson MP, Kunin A et al. Development of a mouse model for sporadic and metastatic colon tumors and its use in assessing drug treatment. Proc Natl Acad Sci U S A 2010; 107: 1565–1570. [PubMed: 20080688]

44. Paul Olson TJ, Hadac JN, Sievers CK, Leystra AA, Deming DA, Zahm CD et al. Dynamic tumor growth patterns in a novel murine model of colorectal cancer. Cancer Prev Res (Phila) 2014; 7: 105–113. [PubMed: 24196829]

45. Sato T, Stange DE, Ferrante M, Vries RG, Van Es JH, Van den Brink S et al. Long-term expansion of epithelial organoids from human colon, adenoma, adenocarcinoma, and Barrett's epithelium. Gastroenterology 2011; 141: 1762–1772. [PubMed: 21889923]

46. Bolger AM, Lohse M, Usadel B. Trimmomatic: a flexible trimmer for Illumina sequence data. Bioinformatics 2014; 30: 2114–2120. [PubMed: 24695404]

47. Kim D, Landmead B, Salzberg SL. HISAT: a fast spliced aligner with low memory requirements. Nat Methods 2015; 12: 357–U121. [PubMed: 25751142]

48. Liao Y, Smyth GK, Shi W. featureCounts: an efficient general purpose program for assigning sequence reads to genomic features. Bioinformatics 2014; 30: 923–930. [PubMed: 24227677]

49. Love MI, Huber W, Anders S. Moderated estimation of fold change and dispersion for RNA-seq data with DESeq2. Genome Biol 2014; 15: 550. [PubMed: 25516281]

50. Mounir M, Lucchetta M, Silva TC, Olsen C, Bontempi G, Chen X et al. New functionalities in the TCGAbiolinks package for the study and integration of cancer data from GDC and GTEx. PLoS Comput Biol 2019; 15: e1006701. [PubMed: 30835723]

51. Anders S, Pyl PT, Huber W. HTSeq--a Python framework to work with high-throughput sequencing data. Bioinformatics 2015; 31: 166–169. [PubMed: 25260700]

Significance:

These findings show that colorectal cancers can arise independent of EGFR even in its presence via IL10-mediated escape from immune surveillance. This discovery provides a new therapeutic approach to inhibit colorectal cancers resistant to EGFR inhibition.

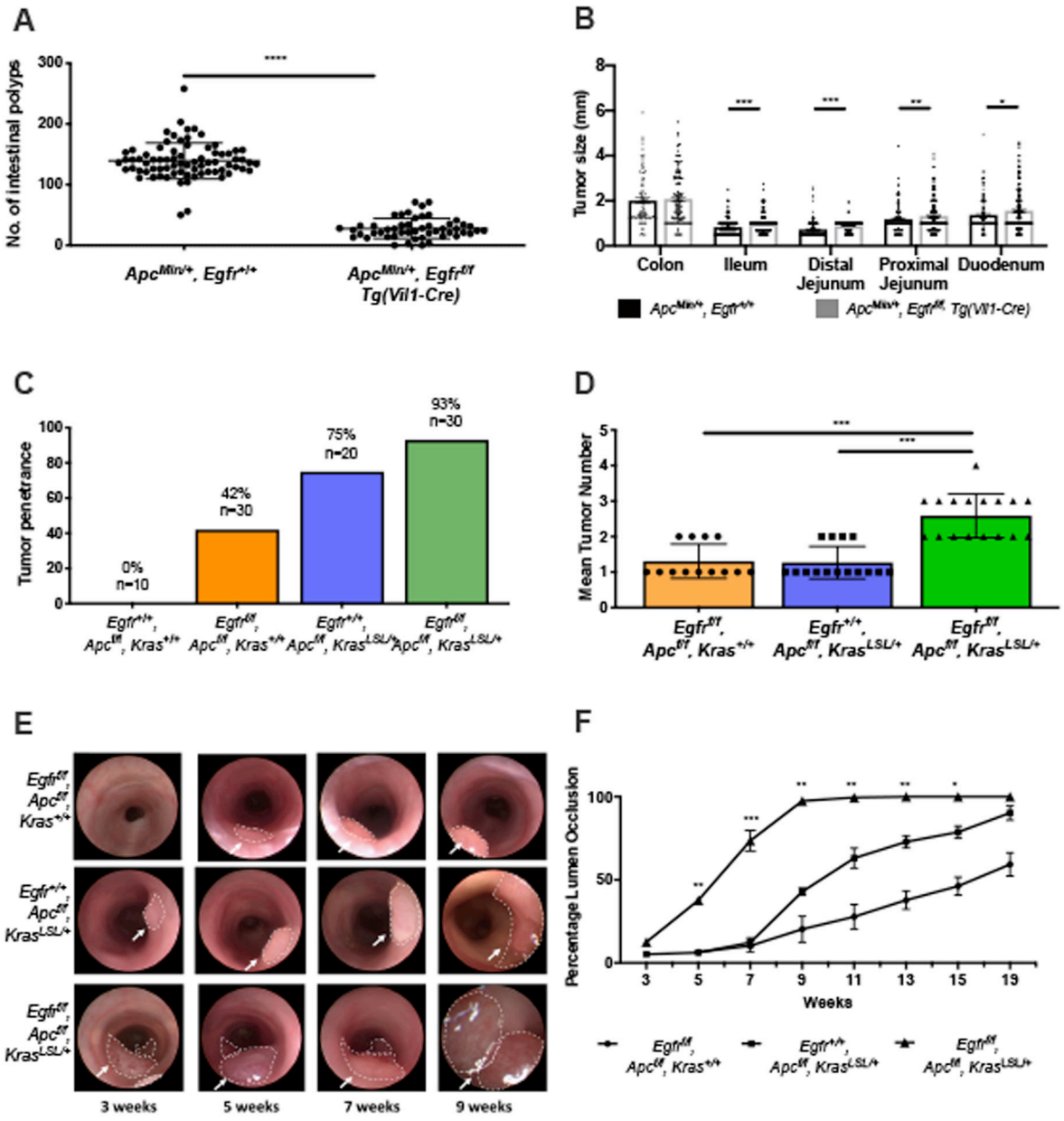

Fig. 1. EGFR-independent intestinal and colonic adenoma development.

a Multiplicity of intestinal polyps is decreased in *$Apc^{Min/+}$, $Egfr^{f/f}$ (Tg(Vil-Cre)* mice. Dots represents polyp number in each 100-day-old mouse. **b** Distribution of polyp sizes show *$Apc^{Min/+}$, $Egfr^{f/f}$ (Tg(Vil-Cre)* polyps are larger than *$Apc^{Min/+}$, $Egfr^{+/+}$*. **c** Colonic polyp penetrance 18 weeks after AdCre induction. **d** Polyp number by endoscopic analysis after AdCre induction. **e** Serial endoscopic images after AdCre administration to the distal colon. **f** Growth curves of AdCre-induced polyps. Data are represented as mean ± SEM. * $p < 0.05$, ** $p < 0.01$, *** $p < 0.001$, **** $p < 0.0001$.

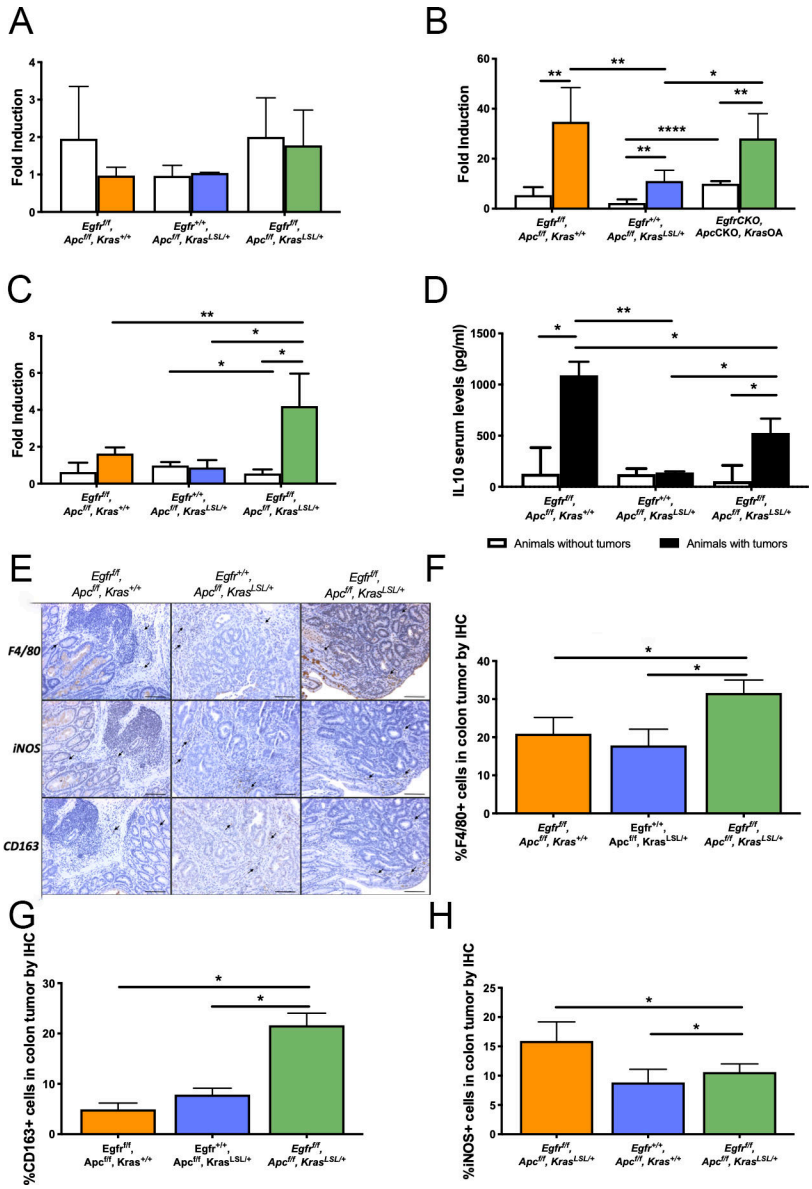

Fig. 2. IL10 signaling activation, in EGFR-independent colon polyps, increased infiltrating immune cells, especially M2-type macrophages.

Transcript levels of **a** *Il10ra*, **b** *Socs3*, and **c** *Il10* measured by qPCR. White bars, mean transcript levels in the adjacent normal tissue; colored bars, mean transcript levels in colon polyps. **d** IL10 levels in serum from mice. White bars, animals without polyps; black bars, animals with polyps. **e** Immunohistochemical staining of macrophage markers. Immunohistochemistry quantification of **f** total, **g** iNOS-positive, and **h** $CD163^{+}$-positive macrophages in induced colon polyps. Data are represented as mean ± SEM. * $p < 0.05$, ** $p < 0.01$, *** $p < 0.001$, **** $p < 0.0001$. All scale bars represent 100um.

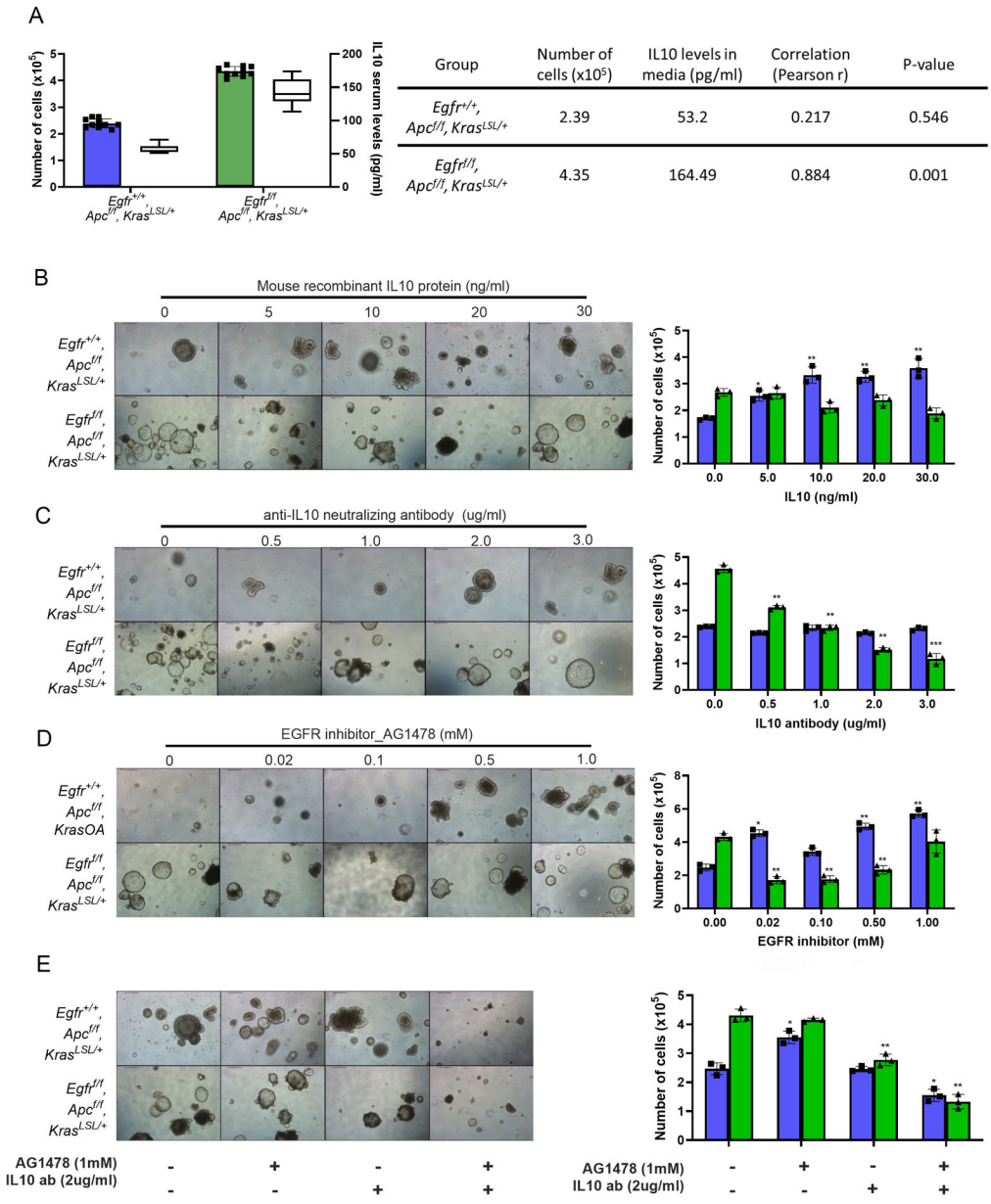

Group	Number of cells (x10^5)	IL10 levels in media (pg/ml)	Correlation (Pearson r)	P-value
Egfr$^{+/+}$, Apc$^{f/f}$, Kras$^{LSL/+}$	2.39	53.2	0.217	0.546
Egfr$^{f/f}$, Apc$^{f/f}$, Kras$^{LSL/+}$	4.35	164.49	0.884	0.001

Fig. 3. Effect of IL10 in cell proliferation in colon organoids.

a Left panel shows number of cells (solid bars, left axis) and IL10 levels in media (white bars, right axis) 24h after seeding. Right panel shows correlation of cell proliferation and IL10 levels in media at 24h after seeding. **b-e** Representative organoid images at 72h post treatment (left panel) and cell proliferation assay (right panel) when organoids were treated with **b** mouse recombinant IL10, **c** IL10 neutralizing antibody, **d** EGFR inhibitor AG1478 and **e** combinatory treatment of AG1478 (1mM) and IL10 antibody (2ug/ml). Equal number of cells (2000 cell/well) were seeded at time 0. Data are represented as mean ± SEM of three experiments performed under the same conditions. Blue bars represent *Egfr$^{+/+}$, Apc$^{f/f}$, Kras$^{LSL/+}$* and green bars represent *Egfr$^{f/f}$, Apc$^{f/f}$, Kras$^{LSL/+}$*. * $p < 0.05$, ** $p < 0.01$, *** $p < 0.001$, **** $p < 0.0001$. All scale bars represent 100um.

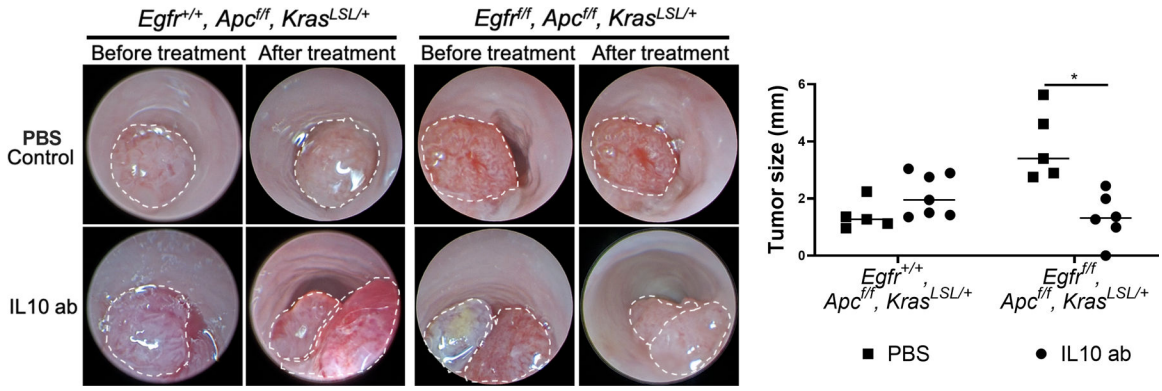

Fig. 4. Anti-IL10 neutralizing antibody treatment.

a Colonoscopic images of colon polyps. Polyp locations are outlined. **b** Polyp sizes measured at necropsy. * $p < 0.05$, ** $p < 0.01$, *** $p < 0.001$, **** $p <$ 0.0001.

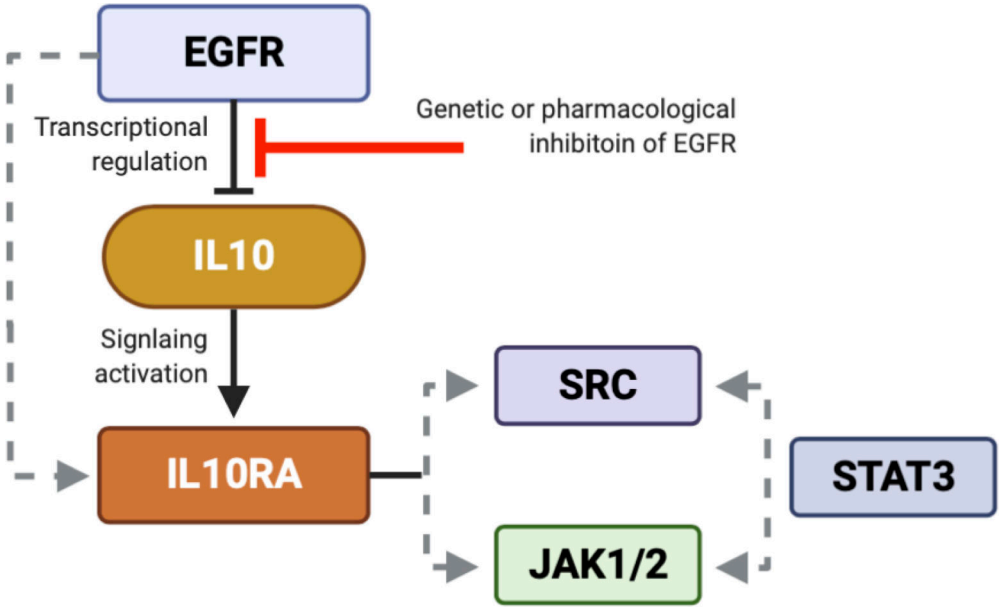

Fig. 5. Proposed EGFR-independent mechanism of colorectal cancer progression.
Black arrows, proven links; grey arrows, proposed interactions from literature.